Journal of Sound and Vibration 329 (2010) 4501–4514

Contents lists available at ScienceDirect

Journal of Sound and Vibration

journal homepage: www.elsevier.com/locate/jsvi

Geometrically nonlinear vibrations of rectangular plates carrying a concentrated mass

M. Amabili *

Department of Mechanical Engineering, McGill University, Macdonald Engineering Building, 817 Sherbrooke Street West, Montreal, Quebéc, Canada H3A 2K6

ARTICLE INFO

Article history:
Received 28 December 2009
Received in revised form
5 April 2010
Accepted 22 April 2010
Handling Editor: M.P. Cartmell
Available online 31 May 2010

ABSTRACT

Nonlinear forced vibrations of rectangular plates carrying a central concentrated mass are studied. The plate is assumed to have immovable edges and rotational springs; numerical results are presented for clamped plates. The Von Kármán nonlinear plate theory is used, but in-plane inertia in both the plate and the mass is retrained. The problem is discretized into a multi-degree-of-freedom (dof) system by using an energy approach and Lagrange equations taking damping into account. A pseudo-arclength continuation method is used in order to obtain numerical solutions. Results are presented as both (i) frequency–amplitude curves and (ii) time domain responses. The effect of gravity and the effect of the consequent initial plate deflection are also investigated.

1. Introduction

Geometrically nonlinear vibrations of plates are particularly interesting since perfectly flat plates present strong hardening-type nonlinearity [1]. Sathyamoorthy [2] reviewed the state-of-art research on nonlinear vibrations of plates until 1987, including some papers dealing with plates carrying concentrated masses. This is an interesting problem that attracted several investigators. Many studies are available on linear vibrations of plates carrying concentrated masses; e.g. see Amabili et al. [3]. However, the following review is limited to nonlinear vibrations.

The first known study on nonlinear (large amplitude) vibrations of plates carrying a mass is due to Chiang and Chen [4], who considered axisymmetric, large amplitude vibrations of a circular plate with inserted concentric rigid mass (not a concentrated mass). The solution was obtained by using the approximate Berger plate equations. As in all the studies available in the literature, only free vibrations were studied.

Ramachandran [5] considered nonlinear vibrations of a rectangular plate with simply supported immovable edges carrying a concentrated mass. The Von Kármán nonlinear plate theory, neglecting in-plane inertia and retaining only a single dof, was used. The assumed mode shape was the first mode of the plate without any mass, i.e. just a rough approximation. Results show that while an increase of the mass largely affects the natural frequency, the frequency–amplitude curve is very little changed. Kanaka Raju [6] studied large amplitude vibrations of circular plates carrying a mass at different positions by using finite elements. Nonlinear vibrations of orthotropic triangular plates carrying a concentrated mass were studied by Karmakar [7] by using the Lagrangian function and neglecting in-plane inertia. Karmakar [8] also

* Tel.: +1 514 398 3068; fax: +1 514 398 7365.
E-mail address: marco.amabili@mcgill.ca
URL: http://people.mcgill.ca/marco.amabili/

0022-460X/$ - see front matter © 2010 Elsevier Ltd. All rights reserved.
doi:10.1016/j.jsv.2010.04.024

studied the large amplitude vibrations of clamped elliptical plates carrying a concentrated mass by using the Von Kármán nonlinear plate theory.

Nonlinear vibrations of clamped orthotropic square plate carrying a mass were studied by Banerjee [9]; the Von Kármán nonlinear plate was used neglecting in-plane inertia and retaining only a single dof. Results were presented only in one figure which , as discussed in Refs. [10,11], has an error in the scale.

Gutiérrez and Laura [12] investigated large amplitude vibrations of rectangular and circular plates carrying a concentrated mass. Also in this case, in-plane inertia was neglected and only a single dof was retained by assuming a mode shape which is the first mode of the plate without any mass attached. Results are obtained for (i) simply supported immovable and (ii) clamped square plates carrying a mass at the center. In both cases, the numerical results show that the nondimensional nonlinear frequency (i.e. the nonlinear frequency divided by the linear one) of the fundamental mode is unchanged by any mass.

The nonlinear transient vibrations of a circular plate with a inserted rigid finite mass were studied by Dumir et al. [13] by using the Von Kármán nonlinear plate theory and neglecting in-plane inertia. The same problem investigated in Ref. [7] was re-investigated by Ghosh [14], but both movable and immovable simply supported edges were considered. In-plane inertia was neglected and only a single dof was retained.

The nonlinear vibrations of a circular plate with a inserted rigid finite mass were studied by Huang and Walker [15], Huang and Huang [16], Huang [17] and Li et al. [18] by using the Kantorovich averaging method [15,18] and the finite element method [16,17].

Khodzhaev and Éshmatov [19] studied nonlinear vibrations of a simply supported, rectangular plate carrying concentrated masses. The plate material is assumed to be viscoelastic. A multi-dof solution is obtained by using the Bubnov–Galerkin method, neglecting in-plane inertia. Results are obtained for free vibration only and presented in the time domain. Therefore, the effect of the vibration amplitude on the vibration frequency is not investigated.

This extensive literature review shows that forced vibrations of plates carrying masses have not been studied yet. Moreover, the limitation of neglecting in-plane inertia is generally used and, in all cases except one, a single dof has been used for rectangular plates.

Nonlinear forced vibrations of rectangular plates carrying a central concentrated mass are studied in the present work. The plate is assumed to have immovable edges and rotational springs; numerical results are presented for clamped plates. The Von Kármán nonlinear plate theory is used, but in-plane inertia in both the plate and the mass is retained. The problem is discretized into a multi-dof system by using an energy approach and Lagrange equations taking damping into account. A pseudo-arclength continuation method is used in order to obtain numerical solutions. Results are presented as both (i) frequency–amplitude curves and (ii) time domain responses. The effect of gravity and the effect of the consequent initial plate deflection are also investigated.

2. Theory

A rectangular isotropic plate of uniform thickness h and in-plane dimensions a and b are considered and a rectangular coordinate system (O; x, y, z) is introduced, where the origin O is assumed at a plate corner on the middle plane of the plate, x and y are the in-plane coordinates and z is the out-of-plane coordinate. At each point of the middle surface of the plate, the displacements in the x, y, z directions are denoted by u, v, w, respectively. Shear deformation and rotary inertia are neglected, as usual for thin plates (but this is legitimate also for moderately thick plates in case of isotropic material). The strain components ε_{xx}, ε_{yy} and γ_{xy} at an arbitrary point of the plate at distance z from the middle surface are related to the middle surface strains $\varepsilon_{x,0}$, $\varepsilon_{y,0}$ and $\gamma_{xy,0}$, and to the changes in the curvature and torsion of the middle surface k_x, k_y and k_{xy} by the following three relations [1]:

$$\varepsilon_{xx} = \varepsilon_{x,0} + zk_x, \tag{1}$$

$$\varepsilon_{yy} = \varepsilon_{y,0} + zk_y, \tag{2}$$

$$\gamma_{xy} = \gamma_{xy,0} + zk_{xy}. \tag{3}$$

Initial geometric imperfections of the rectangular plate associated with zero initial stress are denoted by normal displacement w_0; in-plane initial imperfections and initial stresses are neglected. If Von Kármán hypothesis is used, the following expressions for the middle surface strains and the changes in the curvature and torsion of the middle surface are obtained, namely [1]

$$\varepsilon_{x,0} = \frac{\partial u}{\partial x} + \frac{1}{2}\left(\frac{\partial w}{\partial x}\right)^2 + \frac{\partial w}{\partial x}\,\frac{\partial w_0}{\partial x}, \tag{4}$$

$$\varepsilon_{y,0} = \frac{\partial v}{\partial y} + \frac{1}{2}\left(\frac{\partial w}{\partial y}\right)^2 + \frac{\partial w}{\partial y}\,\frac{\partial w_0}{\partial y}, \tag{5}$$

$$\gamma_{xy,0} = \frac{\partial u}{\partial y} + \frac{\partial v}{\partial x} + \frac{\partial w}{\partial x}\,\frac{\partial w}{\partial y} + \frac{\partial w}{\partial x}\,\frac{\partial w_0}{\partial y} + \frac{\partial w_0}{\partial x}\,\frac{\partial w}{\partial y}. \tag{6}$$

$$k_x = -\frac{\partial^2 w}{\partial x^2}, \tag{7}$$

$$k_y = -\frac{\partial^2 w}{\partial y^2}, \tag{8}$$

$$k_{xy} = -2\frac{\partial^2 w}{\partial x \partial y}. \tag{9}$$

These expressions are in general accurate enough for moderately large vibrations of plates.

2.1. Elastic strain energy

The elastic strain energy U_P of a rectangular isotropic plate, under Kirchhoff's hypothesis $\sigma_{zz}=\tau_{zx}=\tau_{zy}=0$, is given by [1]

$$U_P = \frac{1}{2}\int_0^a\int_0^b\int_{-h/2}^{h/2}(\sigma_{xx}\varepsilon_{xx}+\sigma_{yy}\varepsilon_{yy}+\tau_{xy}\gamma_{xy})dx\,dy\,dz, \tag{10}$$

where σ_{xx}, σ_{yy} and τ_{xy} are the Kirchhoff stresses and ε_{xx}, ε_{yy} and γ_{xy} are Green's strains. The Kirchhoff stresses are related to the Green's strains within the limit of elasticity of the plate's material

$$\sigma_{xx} = \frac{E}{1-\nu^2}(\varepsilon_{xx}+\nu\varepsilon_{yy}), \quad \sigma_{yy} = \frac{E}{1-\nu^2}(\varepsilon_{yy}+\nu\varepsilon_{xx}), \ \tau_{xy} = \frac{E}{2(1+\nu)}\gamma_{xy}, \tag{11–13}$$

where E is the Young's modulus and ν is the Poisson's ratio. The simplicity of Eq. (10) is due to the Lagrangian description of the plate, which allows integration over the plate in the original undeformed configuration.

2.2. Kinetic energy and virtual work of external forces

The kinetic energy T_P of a rectangular plate carrying a central concentrated mass M, by neglecting rotary inertia, is given by

$$T_P = \frac{1}{2}M(\dot{u}^2+\dot{v}^2+\dot{w}^2)|_{x=a/2,y=b/2}+\frac{1}{2}\rho_P h\int_0^a\int_0^b(\dot{u}^2+\dot{v}^2+\dot{w}^2)dx\,dy, \tag{14}$$

where ρ_p is the mass density of the plate. In Eq. (14) the overdot denotes a time derivative.

The virtual work W done by the external forces is written as

$$W = \int_0^a\int_0^b(q_x u+q_y v+q_z w)dx\,dy, \tag{15}$$

where q_x, q_y and q_z are the distributed forces per unit area acting in x-, y- and z-direction, respectively. In the present study, a single harmonic force orthogonal to the plate is considered; therefore, $q_x=q_y=0$. In some cases, the mass M and the plate are subjected to a gravity field, which is assumed to have the z-direction. The external distributed load q_z is applied to the plate, due to the concentrated force $\tilde{f}$, is given by

$$q_z = \tilde{f}\delta(y-\tilde{y})\delta(x-\tilde{x})\cos(\omega t), \tag{16}$$

where ω is the excitation frequency, t is the time, δ is the Dirac delta function, $\tilde{f}$ is the force magnitude positive in z-direction; $\tilde{x}$ and $\tilde{y}$ give the position of the point of application of the force. The contribution given by the vertical gravity field to q_z is a static pressure having the following distribution:

$$q_z = Mg\delta(y-b/2)\delta(x-a/2)+\rho_P hg, \tag{17}$$

where g is the gravity acceleration.

2.3. Boundary conditions and discretization

Plates with fixed edges are considered. The following boundary conditions are introduced for plates with fixed edges:

$$u=v=w=w_0=0, \quad M_x = \mp k\,\partial w/\partial x \quad \text{at } x=0,a, \tag{18a–e}$$

$$u=v=w=w_0=0, \quad M_y = \mp k\,\partial w/\partial y \quad \text{at } y=0,b, \tag{19a–e}$$

where k is the stiffness per unit length of the elastic, distributed rotational springs placed at the four edges, $x=0$, a and $y=0$, b; the minus sign in Eqs. (18e) and (19e) applies at the boundaries $x=0$ and $y=0$. Equations (18e) and (19e) represent the case of an elastic rotational constraint at the shell edges. They give any rotational constraint from zero bending moment ($M_x=0$ and $M_y=0$, unconstrained rotation, obtained for $k=0$) to perfectly clamped plate ($\partial w/\partial x=0$ and $\partial w/\partial y=0$, obtained as limit for $k\to\infty$), according to the value of k.

The displacements u, v and w are expanded by using the following expressions, which satisfy identically the geometric boundary conditions (18a–c) and (19a–c):

$$u(x,y,t)=\sum_{i=1}^{I}\sum_{n=1}^{N}u_{2i,n}(t)\sin(2i\pi x/a)\sin(n\pi y/b), \tag{20a}$$

$$v(x,y,t)=\sum_{i=1}^{I}\sum_{n=1}^{N}v_{i,2n}(t)\sin(i\pi x/a)\sin(2n\pi y/b), \tag{20b}$$

$$w(x,y,t)=\sum_{i=1}^{\hat{I}}\sum_{n=1}^{\hat{N}}w_{i,n}(t)\sin(i\pi x/a)\sin(n\pi y/b), \tag{20c}$$

where i and n are the numbers of half-waves in x- and y- direction, respectively, and t is the time; $u_{i,n}(t)$, $v_{i,n}(t)$ and $w_{i,n}(t)$ are the generalized coordinates, which are unknown functions of t. I and N indicate the terms necessary in the expansion of the in-plane displacements and, in general, are larger than $\hat{I}$ and $\hat{N}$, respectively, which indicate the terms in the expansion of w.

On the other hand, Eqs. (18e) and (19e) can be rewritten in the following form:

$$M_x=\frac{Eh^3}{12(1-\nu^2)}(k_x+\nu\,k_y)=\mp k\,\partial w/\partial x \quad \text{at } x=0,a, \tag{21}$$

$$M_y=\frac{Eh^3}{12(1-\nu^2)}(k_y+\nu k_x)=\mp k\partial w/\partial y \quad \text{at } y=0,b. \tag{22}$$

These boundary conditions are nongeometric. For this reason, Eqs. (20) do not have to satisfy Eqs. (21) and (22) since they are automatically satisfied by energy minimization. If k is different from zero, an additional potential energy stored by the elastic rotational springs at the plate edges must be added to the potential energy of the plate. This potential energy U_R is given by

$$U_R=\frac{1}{2}\int_0^b k\left\{\left[\left(\frac{\partial w}{\partial x}\right)_{x=0}\right]^2+\left[\left(\frac{\partial w}{\partial x}\right)_{x=a}\right]^2\right\}\mathrm{d}y+\frac{1}{2}\int_0^a k\left\{\left[\left(\frac{\partial w}{\partial y}\right)_{y=0}\right]^2+\left[\left(\frac{\partial w}{\partial y}\right)_{y=b}\right]^2\right\}\mathrm{d}x. \tag{23}$$

In order to simulate clamped edges in numerical calculations, a very high value of the stiffness k must be assumed. This approach is usually referred as the artificial spring method [1,20], which can be regarded as a variant of the classical penalty method. The values of the spring stiffness simulating a clamped plate can be obtained by studying the convergence of the natural frequencies of the linearized solution by increasing the value of k. In fact, it was found that the natural frequencies of the system converge asymptotically with those of a clamped plate when k becomes very large.

Initial geometric imperfections of the rectangular plate are considered only in the z-direction. They are associated with zero initial stress. The imperfection w_0 is expanded in the same form of w, i.e. in a double Fourier sine series satisfying the boundary conditions (18d) and (19d) at the plate edges

$$w_0(x,y)=\sum_{i=1}^{\tilde{I}}\sum_{n=1}^{\tilde{N}}A_{i,n}\sin(i\pi x/a)\sin(n\pi y/b), \tag{24}$$

where $A_{i,n}$ are the modal amplitudes of imperfections; $\tilde{N}$ and $\tilde{I}$ are integers indicating the number of terms in the expansion. Geometric imperfections are introduced here but they are not investigated numerically in the present study.

2.4. Lagrange equations of motion

The nonconservative damping forces are assumed to be of viscous type and are taken into account by using the Rayleigh's dissipation function

$$F=\frac{1}{2}c\int_0^a\int_0^b(\dot{u}^2+\dot{v}^2+\dot{w}^2)\mathrm{d}x\,\mathrm{d}y, \tag{25}$$

where c has a different value for each term of the mode expansion. Simple calculations give

$$F=\frac{1}{2}(ab/4)\left[\sum_{i=1}^{\hat{I}}\sum_{n=1}^{\hat{N}}c_{i,n}\dot{w}_{i,n}^2+\sum_{i=1}^{I}\sum_{n=1}^{N}c_{i,n}\dot{u}_{i,n}^2+\sum_{i=1}^{I}\sum_{n=1}^{N}c_{i,n}\dot{v}_{i,n}^2\right]. \tag{26}$$

The damping coefficient $c_{i,n}$ is related to modal damping ratio (in this case it is a damping ratio of the generalized coordinate), that can be evaluated from experiments, by $\varsigma_{i,n}=\tilde{c}_{i,n}/(2\mu_{i,n}\omega_{i,n})$, where $\omega_{i,n}$ is the natural circular frequency of mode (i,n) and $\tilde{c}_{i,n}$ is the damping coefficient obtained after diagonalization of the mass matrix (see Section 2.5). $\mu_{i,n}$ is the mass associated with this generalized coordinate after diagonalization of the mass matrix.

The following notation is introduced for brevity:

$$\mathbf{q}=\{u_{i,n},v_{i,n},w_{i,n}\}^{\mathrm{T}},\quad i=1,\ldots,I\quad\text{or}\quad\hat{I}\quad\text{and}\quad n=1,\ldots,N\ \text{or}\ \hat{N}. \tag{27}$$

The generic element of the time-dependent vector $\mathbf{q}$ is referred to as q_j, which is the generalized coordinate; the dimension of $\mathbf{q}$ is $\overline{N}$, which is the number of dof used in the mode expansion.

The generalized forces Q_j are obtained by differentiation of the Rayleigh's dissipation function and of the virtual work done by external forces

$$Q_j=-\frac{\partial F}{\partial\dot{q}_j}+\frac{\partial W}{\partial q_j}. \tag{28}$$

The Lagrange equations of motion are

$$\frac{\mathrm{d}}{\mathrm{d}t}\left(\frac{\partial T_P}{\partial\dot{q}_j}\right)-\frac{\partial T_P}{\partial q_j}+\frac{\partial U}{\partial q_j}=Q_j,\quad j=1,\ldots,\overline{N}, \tag{29}$$

where $\partial T_P/\partial q_j=0$ and the potential energy is given by $U=U_P+U_R$, where U_P is given by Eq. (10) and U_R by Eq. (23). These second-order equations have very long expressions containing quadratic and cubic nonlinear terms. In particular, the only term containing nonlinearities is

$$\frac{\partial U}{\partial q_j}=\sum_{k=1}^{\overline{N}}f_{m,j}q_m+\sum_{m,k=1}^{\overline{N}}f_{m,k,j}q_mq_k+\sum_{m,k,l=1}^{\overline{N}}f_{m,k,l,j}q_mq_kq_l, \tag{30}$$

where coefficients f have long expressions that also include geometric imperfections. Quadratic nonlinearities of the type q_m^2 (in particular for $q_m=w_{i,n}$) are never present in the equations of motion of perfect flat plates. This is a difference with respect to curved panels and it is physically explained by the fact that no different displacement is observed for flat plates

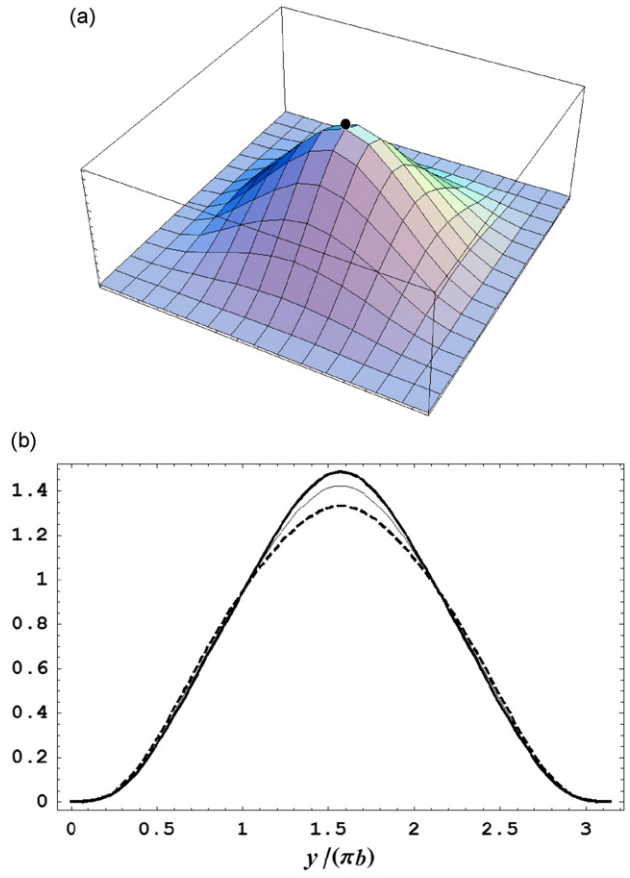

Fig. 1. Shape of the fundamental mode of the plate with and without concentrated mass neglecting gravity. (a) A 3-D representation for mass of 0.1 kg; (b) cross-section at $x=a/2$; –, plate without mass; ——, plate with mass 0.025 kg and ▬▬, plate with mass 0.1 kg.

in z- and $-z$-direction, due to the symmetry. Presence of quadratic nonlinearities is the reason for significant asymmetric displacement in z and $-z$ that is observed in the results in case of initial geometric imperfections or mass load in gravity field.

2.5. Inertial decoupling of the equations of motion

For plates with concentrated mass, inertial coupling arises in the equations of motion so that they cannot be immediately transformed in the form required for numerical integration. In particular, the equations of motion take the following form:

$$\mathbf{M}\ddot{\mathbf{q}}+\mathbf{C}\dot{\mathbf{q}}+[\mathbf{K}+\mathbf{N_2}(\mathbf{q})+\mathbf{N_3}(\mathbf{q},\mathbf{q})]\mathbf{q}=\mathbf{f_0}\cos(\omega t)+\mathbf{f_1}, \tag{31}$$

where $\mathbf{M}$ is the nondiagonal mass matrix of dimension $\overline{N}\times\overline{N}$ ($\overline{N}$ being the number of dof), $\mathbf{C}$ is the damping matrix, $\mathbf{K}$ is the linear stiffness matrix, which does not present terms involving $\mathbf{q}$, $\mathbf{N_2}$ is the matrix that involves linear terms in $\mathbf{q}$, therefore, giving the quadratic nonlinear stiffness terms, $\mathbf{N_3}$ is a matrix that involves quadratic terms in $\mathbf{q}$, therefore, giving the cubic nonlinear stiffness terms, $\mathbf{f_0}$ is the vector of excitation amplitudes, $\mathbf{f_1}$ is the vector of the gravity load and $\mathbf{q}$ is the vector of the $\overline{N}$ generalized coordinates, defined in Eq. (27). In particular, by using Eq. (30), the generic elements $k_{m,j}$, $n_{2m,j}$ and $n_{3m,j}$, of the matrices $\mathbf{K}$, $\mathbf{N_2}$ and $\mathbf{N_3}$, respectively, are given by

$$k_{m,j}=f_{m,j},\quad n_{2_{m,j}}(\mathbf{q})=\sum_{k=1}^{\overline{N}}f_{m,k,j}q_k,\quad n_{3_{m,j}}(\mathbf{q},\mathbf{q})=\sum_{k,l=1}^{\overline{N}}f_{m,k,l,j}q_kq_l. \tag{32a–c}$$

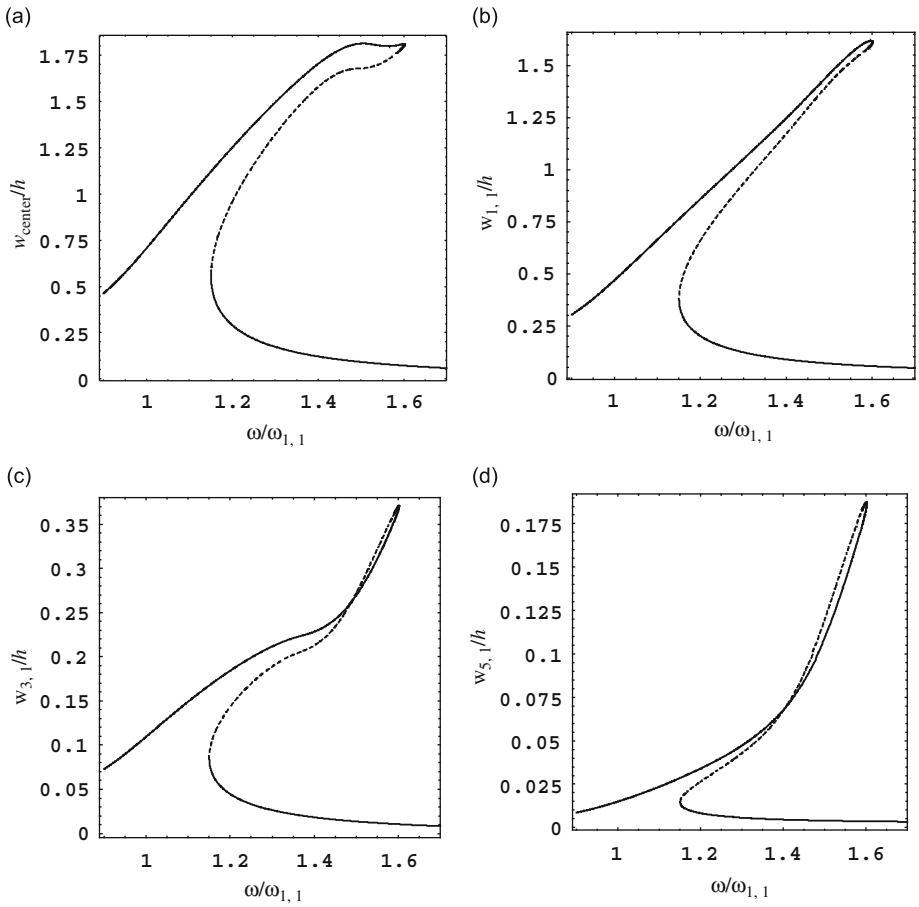

Fig. 2. Frequency-response curve of the plate with concentrated mass of 0.025 kg; excitation at the center with $\tilde{f}=0.482$ N in the frequency neighborhood of the first resonance; results show the first harmonic only; $\zeta_{1,1}=0.012$; 39 dofs; ——, stable solution; - -, unstable solution. (a) Response at the center of the plate; (b) maximum of the generalized coordinate $w_{1,1}$; (c) maximum of the generalized coordinate $w_{3,1}$; (d) maximum of the generalized coordinate $w_{5,1}$; (e) maximum of the generalized coordinate $w_{1,3}$; (f) maximum of the generalized coordinate $w_{3,3}$; (g) maximum of the generalized coordinate $w_{1,5}$ and (h) maximum of the generalized coordinate $u_{2,1}$.

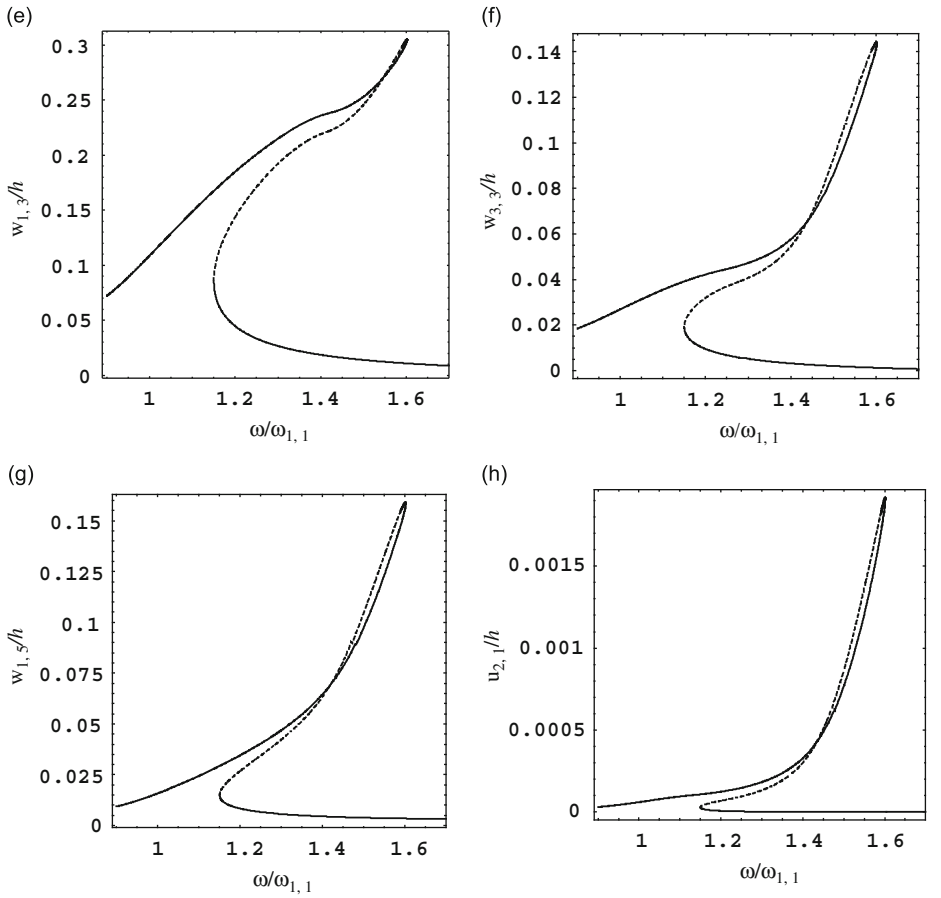

Fig. 2. (*Continued*)

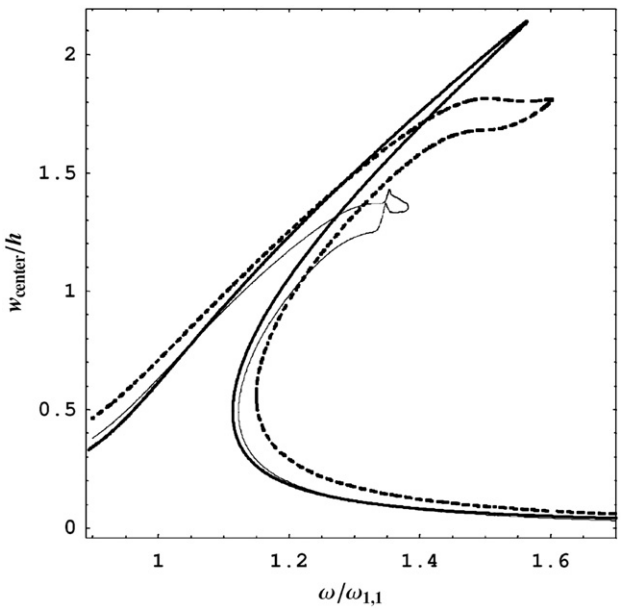

Fig. 3. Comparison of frequency-responses at the center of plates with and without concentrated masses; $\zeta_{1,1}$=0.012; ——, plate without mass, $\tilde{f} = 0.392$ N; - - , plate with mass 0.025 kg, $\tilde{f} = 0.482$ N; ▬▬, plate with mass 0.1 kg, $\tilde{f} = 0.303$ N.

Eq. (31) is pre-multiplied by $\mathbf{M}^{-1}$ in order to diagonalize the mass matrix, as a consequence that the matrix $\mathbf{M}$ is always invertible; the result is

$$\mathbf{I}\,\ddot{\mathbf{q}}+\mathbf{M}^{-1}\mathbf{C}\,\dot{\mathbf{q}}+[\mathbf{M}^{-1}\mathbf{K}+\mathbf{M}^{-1}\mathbf{N_2}(\mathbf{q})+\mathbf{M}^{-1}\mathbf{N_3}(\mathbf{q},\mathbf{q})]\mathbf{q}=\mathbf{M}^{-1}\mathbf{f_0}\cos(\omega t)+\mathbf{M}^{-1}\mathbf{f_1}, \tag{33}$$

where $\mathbf{I}$ is the unit matrix. Eq. (33) can be rewritten in the following form:

$$\mathbf{I}\,\ddot{\mathbf{q}}+\tilde{\mathbf{C}}\,\dot{\mathbf{q}}+[\tilde{\mathbf{K}}+\mathbf{M}^{-1}\mathbf{N_2}(\mathbf{q})+\mathbf{M}^{-1}\mathbf{N_3}(\mathbf{q},\mathbf{q})]\,\mathbf{q}=\tilde{\mathbf{f}}_{\mathbf{0}}\cos(\omega t)+\tilde{\mathbf{f}}_{\mathbf{1}}, \tag{34}$$

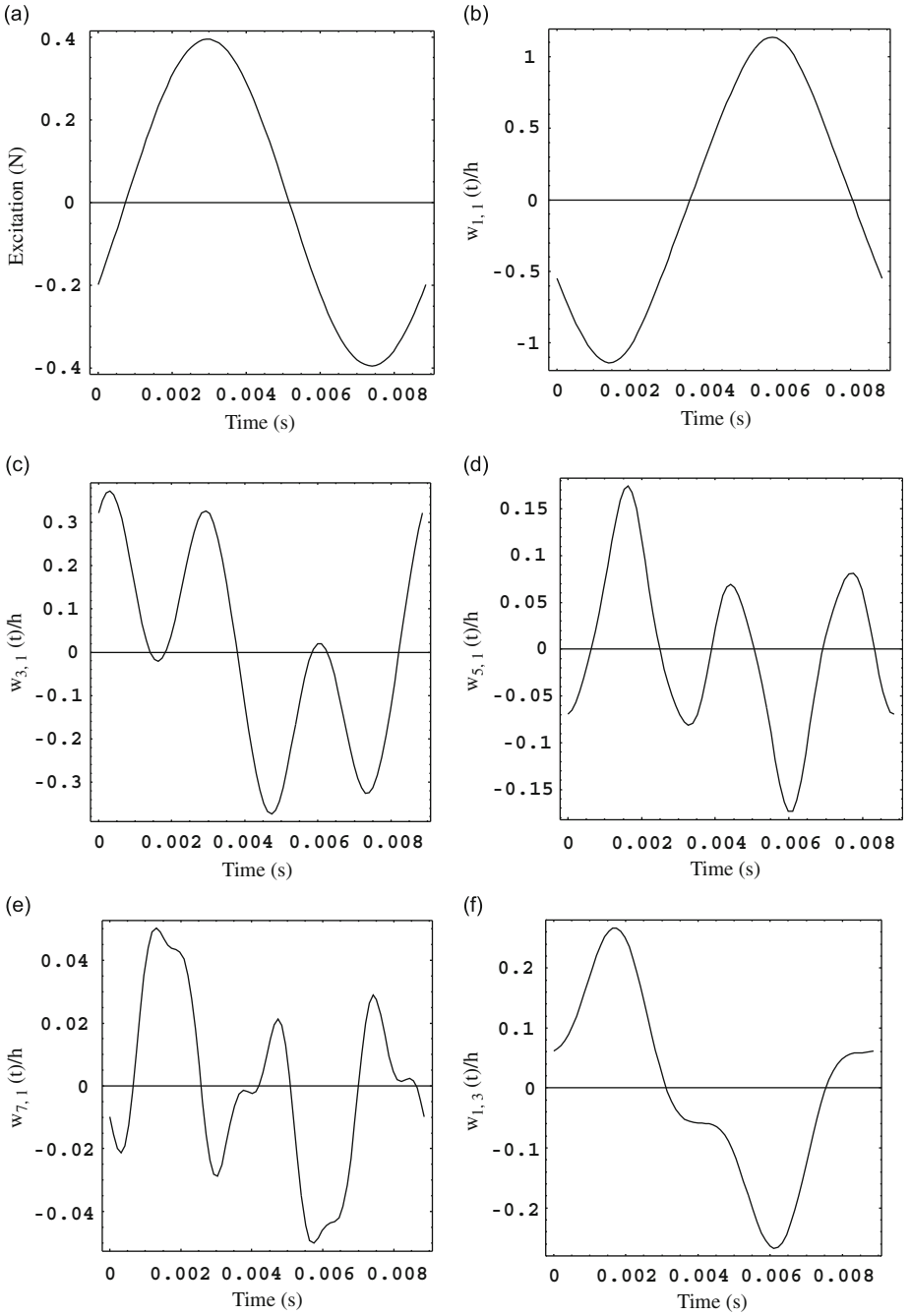

Fig. 4. Time response at the resonance peak of the plate without concentrated mass; $\zeta_{1,1}$=0.012. (a) Force excitation; (b) maximum of the generalized coordinate $w_{1,1}$; (c) maximum of the generalized coordinate $w_{3,1}$; (d) maximum of the generalized coordinate $w_{5,1}$; (e) maximum of the generalized coordinate $w_{7,1}$; (f) maximum of the generalized coordinate $w_{1,3}$; (g) maximum of the generalized coordinate $w_{3,3}$; (h) maximum of the generalized coordinate $u_{2,1}$; (i) response at the center of the plate; (j) amplitude of the frequency spectrum of $w_{1,1}$; (k) amplitude of the frequency spectrum of $w_{3,1}$ and (l) amplitude of the frequency spectrum of response at the plate center.

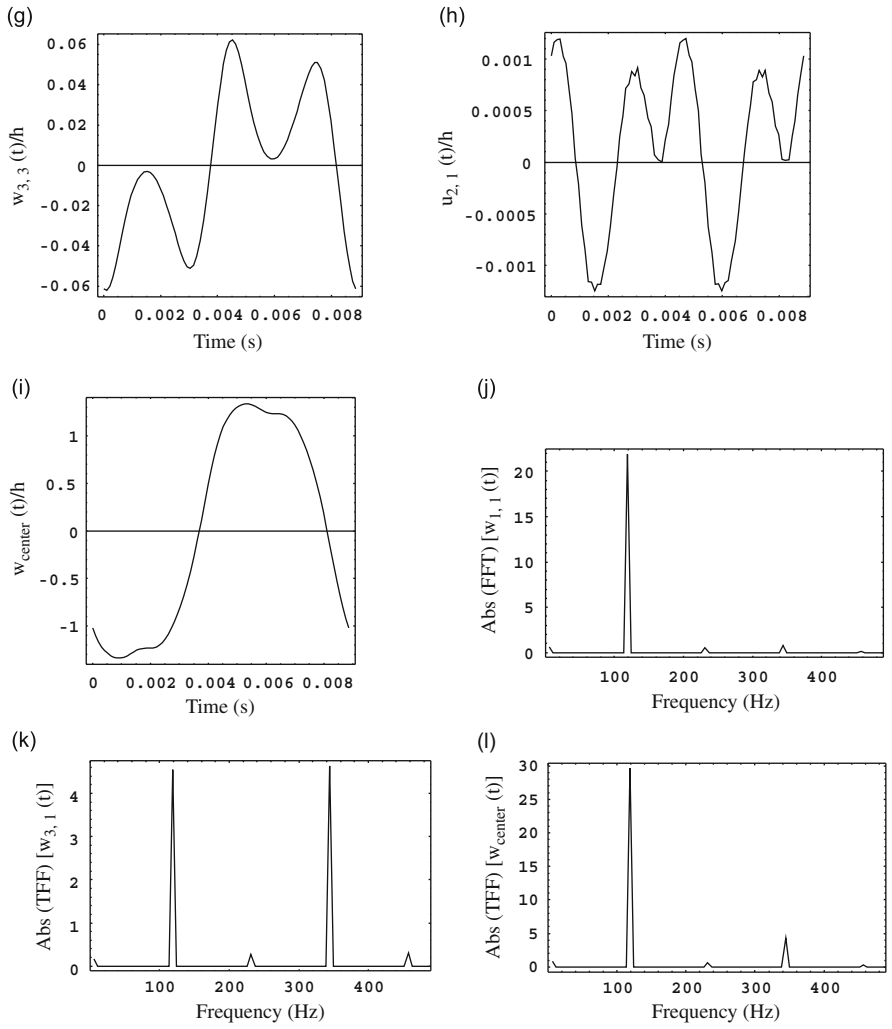

Fig. 4. (*Continued*)

where

$$\tilde{\mathbf{C}} = \mathbf{M}^{-1}\mathbf{C}, \quad \tilde{\mathbf{K}} = \mathbf{M}^{-1}\mathbf{K}, \quad \tilde{\mathbf{f}}_{\mathbf{0}} = \mathbf{M}^{-1}\mathbf{f}_{\mathbf{0}} \quad \text{and} \quad \tilde{\mathbf{f}}_{\mathbf{1}} = \mathbf{M}^{-1}\mathbf{f}_{\mathbf{1}}. \tag{35a–d}$$

Here, modal damping is assumed for simplicity, so that $\tilde{\mathbf{C}}$ is a diagonal matrix. Eq. (34) is in the form suitable for numerical integration.

3. Numerical results

The generic *j*th Lagrange equation is transformed in two first-order equations; this is possible since the equations have been decoupled with respect to inertia. A non-dimensionalization of variables is also performed for computational convenience; the frequencies are divided by the natural radian frequency $\omega_{i,n}$ of the mode (i, n) investigated, and the vibration amplitudes are divided by the plate thickness h. The resulting $2 \times \overline{N}$ equations are studied by using the software AUTO 97 [21] for continuation and bifurcation analysis of nonlinear ordinary differential equations. The software AUTO is capable of continuation of the solution, bifurcation analysis and branch switching by using pseudo-arclength continuation [1] and collocation methods. In particular, the plate response under harmonic excitation has been studied by using an analysis in three steps: (i) for zero excitation, the static load due to the gravity acceleration is used as bifurcation parameter; the solution has been started at zero static load where the solution is the trivial undisturbed configuration of the plate and has been continued up to reach the desired magnitude of the static load; (ii) then, the excitation frequency has been fixed far enough from resonance and the magnitude of the excitation has been used as bifurcation parameter; the

solution has been continued using as restarting point the deformed configuration obtained at step (i); (iii) when the desired magnitude of excitation has been reached, the solution has been continued by using the excitation frequency as bifurcation parameter.

Calculations have been performed for a rectangular AISI 304 stainless steel plate with the following dimensions and material properties: a=0.25 m, b=0.24 m, h=0.0005 m, $E=198\times10^9$ Pa, ρ=7850 kg/m^3 and ν=0.3. This plate has fundamental mode (i=1, n=1) with radian frequency $\omega_{1,1}=78.3\times2\pi$ rad/s (with a model with 108 dof) for clamped edges simulated with $k=10^5$ N/rad. The plate is considered for harmonic excitation around the fundamental resonance, at the plate center (at $x=a/2$ and $y=b/2$), of magnitude $\tilde{f}=0.392$ N, assuming modal damping $\zeta_{1,1}$=0.012 (the same damping ratio is assumed for all the generalized coordinates). Present results have been obtained by using a model with 39 dofs, i.e.

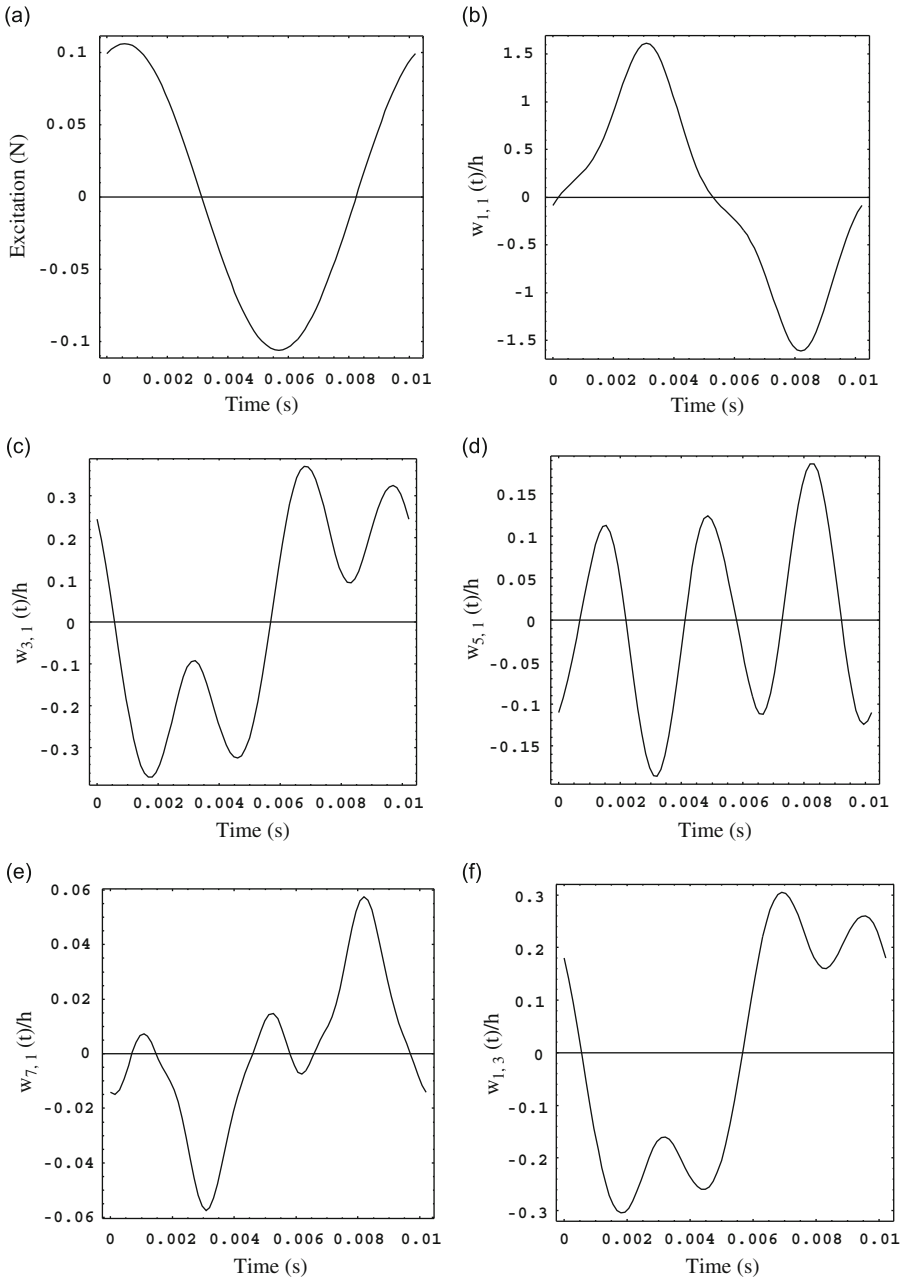

Fig. 5. Time response at the resonance peak of the plate with concentrated mass of 0.025 kg; $\zeta_{1,1}$=0.012. (a) Force excitation; (b) maximum of the generalized coordinate $w_{1,1}$; (c) maximum of the generalized coordinate $w_{3,1}$; (d) maximum of the generalized coordinate $w_{5,1}$; (e) maximum of the generalized coordinate $w_{7,1}$; (f) maximum of the generalized coordinate $w_{1,3}$; (g) maximum of the generalized coordinate $w_{3,3}$; (h) maximum of the generalized coordinate $u_{2,1}$; (i) response at the center of the plate; (j) amplitude of the frequency spectrum of $w_{1,1}$; (k) amplitude of the frequency spectrum of $w_{3,1}$ and (l) amplitude of the frequency spectrum of response at the plate center.

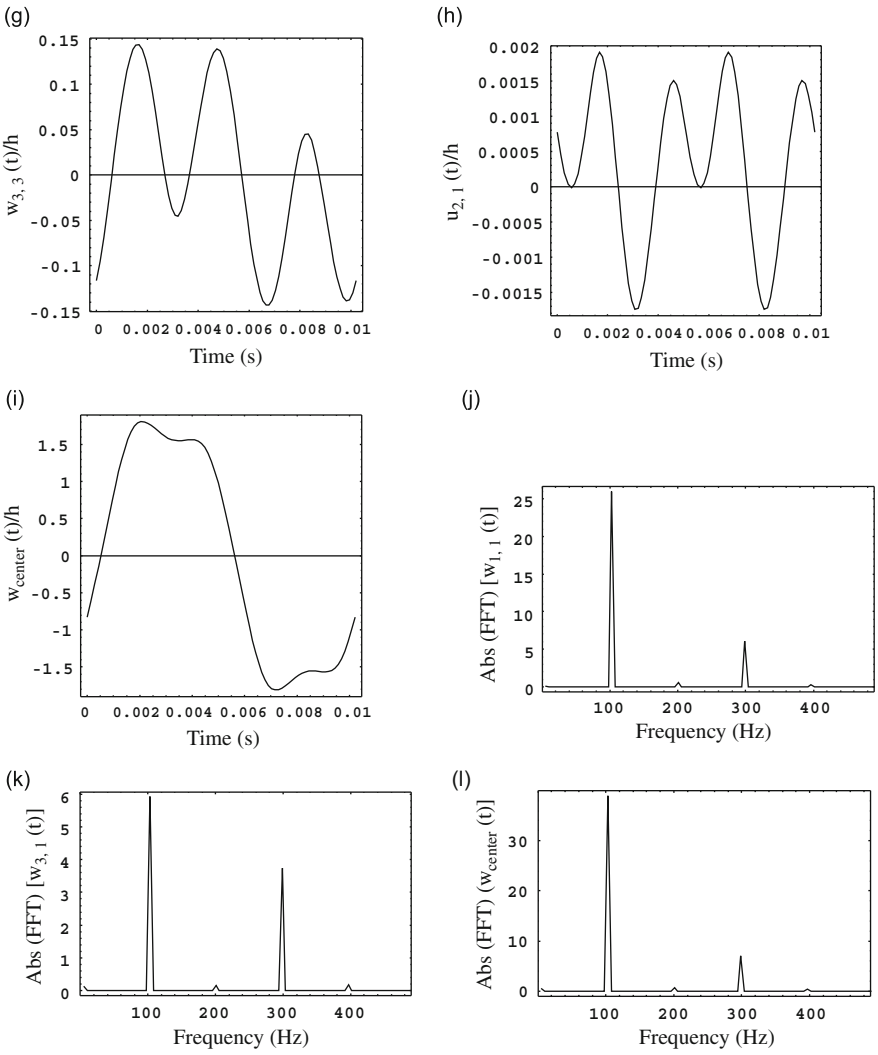

Fig. 5. (*Continued*)

with 39 generalized coordinates. In particular, they are: $w_{1,1}$, $w_{3,1}$, $w_{5,1}$, $w_{7,1}$, $w_{1,3}$, $w_{3,3}$, $w_{5,3}$, $w_{7,3}$, $w_{1,5}$, $w_{3,5}$, $w_{5,5}$, $w_{1,7}$, $w_{3,7}$, $u_{2,1}$, $u_{4,1}$, $u_{6,1}$, $u_{8,1}$, $u_{2,3}$, $u_{4,3}$, $u_{6,3}$, $u_{8,3}$, $u_{2,5}$, $u_{4,5}$, $u_{6,5}$, $u_{2,7}$, $u_{4,7}$, $v_{1,2}$, $v_{3,2}$, $v_{5,2}$, $v_{7,2}$, $v_{1,4}$, $v_{3,4}$, $v_{5,4}$, $v_{7,4}$, $v_{1,6}$, $v_{3,6}$, $v_{5,6}$, $v_{1,8}$, $v_{3,8}$. This model has been proved to be accurate for plates without masses by Amabili [22]. Then, two cases with concentrated mass at the center of the plate have been considered. The first case is a concentrated mass of 0.025 kg; this mass is small enough to represent added sensors (piezoelectric load cell and accelerometer) during experimental modal analysis. The radian frequency of the plate with the small mass attached is $\omega_{1,1}=59.1\times 2\pi$ rad/s and it has been studied with excitation $\tilde{f}=0.482$ N. Finally, a plate carrying a larger concentrated mass has been studied. The mass is 0.1 kg, the radian frequency $\omega_{1,1}=38.2\times 2\pi$ rad/s and the excitation $\tilde{f}=0.303$ N. All the other parameters (damping, dof and stiffness of rotational springs) are unchanged.

3.1. Numerical results neglecting gravity

Fig. 1 shows the shape of the fundamental mode ($i=1$ and $n=1$) of the clamped plate without and with a concentrated mass of 0.025 and 0.1 kg. Fig. 1(b) clearly shows that the effect of the mass is that of slightly concentrating the movement at the mass location, i.e. at the center of the plate. This is obtained by solving the linear eigenvalue problem.

The maximum plate oscillation at the center of the plate carrying a concentrated mass of 0.025 kg is presented in Fig. 2(a) for harmonic excitation of 0.482 N applied at the center of the plate in the frequency neighborhood of the fundamental mode. It is evident that the clamped boundary condition gives strong hardening-type nonlinearity. The strange behavior near the response peak is due to two 3:1 internal resonances: (i) between mode (1,1) and the second mode for $\omega=1.29\times\omega_{1,1}$ and (ii) between mode (1,1) and the third mode for $\omega=1.68\times\omega_{1,1}$. The contributions of the most

significant generalized coordinates to the response shown in Fig. 2(a) are plotted in Fig. 2(b–h), where internal resonances are evident.

The comparison of the maximum plate oscillation at the center of the plate without mass and with concentrated mass (0.025 and 0.1 kg) is shown in Fig. 3. Results show that increasing the concentrated mass, the system changes slightly the trend of nonlinearity, specifically decreasing the hardening-type nonlinearity. However, the difference in the trend of nonlinearity is small. The cases without mass and with smaller mass (0.025 kg) present a rounded tip at the resonance peak due to internal resonances, while the case with larger concentrated mass of 0.1 kg does not present internal resonances, so the tip of the response is sharper. Also interesting is that the concentrated mass is amplifying the response at the mass location, more than in the small amplitude (linear) vibrations.

Results presented in Fig. 3 are in good agreement with the free vibration results obtained by Gutiérrez and Laura [12] for clamped square plates. In fact, for clamped square plates without mass or with any mass at their center, they found a frequency of the fundamental mode of $1.066\omega_{1,1}$ for vibration amplitude $0.6h$, and a frequency $1.17\omega_{1,1}$ for vibration amplitude h. Since our plate is almost square (b/a=0.96), our results can be practically directly compared to those obtained by Gutiérrez and Laura [12]. The curve showing the free vibration frequency as a function of the vibration amplitude is named backbone curve and it lies "in the middle" of the forced response curve shown in Fig. 3. The backbone curve obtained by Gutiérrez and Laura [12] is close enough to the middle of the forced response curves shown in Fig. 3 for any of the three cases considered with different masses and no mass; this is a good validation of the present approach.

The time response at the resonance peak of the clamped plate without concentrated mass is shown in Fig. 4 for the main generalized coordinates and the response at the center of the plate, together with the excitation and the frequency spectrum. Results show that the main generalized coordinate $w_{1,1}$ has almost no contribution of higher harmonics, which appear on the other coordinates. Anyway, the plate oscillation at the center has just a smaller contribution of the third harmonics. On the other hand, Fig. 5 shows a much larger contribution of the third harmonic to both $w_{1,1}$ and the oscillation at the center in case of concentrated mass of 0.025 kg. Finally, since no internal resonances are activated, the time response at the resonance peak in case of mass 0.1 kg has practically no contribution of higher harmonics on both $w_{1,1}$ and the oscillation at the center of the plate, as shown in Fig. 6.

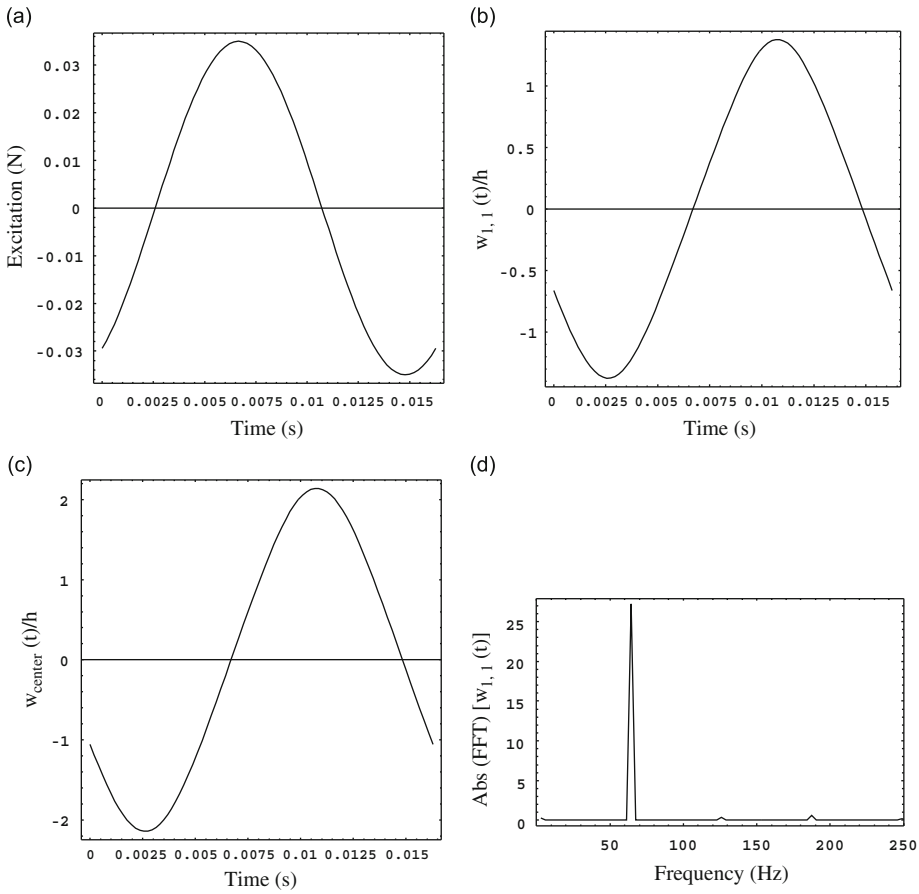

Fig. 6. Time response at the resonance peak of the plate with concentrated mass of 0.1 kg; $\zeta_{1,1}$=0.012. (a) Force excitation; (b) maximum of the generalized coordinate $w_{1,1}$; (c) response at the center of the plate and (d) amplitude of the frequency spectrum of $w_{1,1}$.

3.2. Numerical results in vertical gravity field

A vertical gravity field is now assumed to be acting on the plate and the concentrated mass, with direction opposite to the bending deflection w. The gravity acceleration g=9.81 m/s^2 is assumed. Here, the plate with mass of 0.1 kg is considered since this is the case where the gravity plays the larger role. As a consequence of the gravity acceleration, the plate has an initial static deflection. The forced vibration is now calculated starting from the initial bended configuration of the plate, which is no longer plane and unstressed before vibrating. The maximum amplitude of the main generalized coordinate $w_{1,1}$ is plotted in Fig. 7(a) versus the results of the same case neglecting the gravity acceleration. The response of the plate, due to the initial deflection, is less hardening than the one obtained neglecting it. It also starts from a value below zero since there is an initial negative deflection. Moreover, the natural frequency is slightly increased to about 4%, due to the initial deformation. The minimum of the same generalized coordinate is shown in Fig. 7(b).

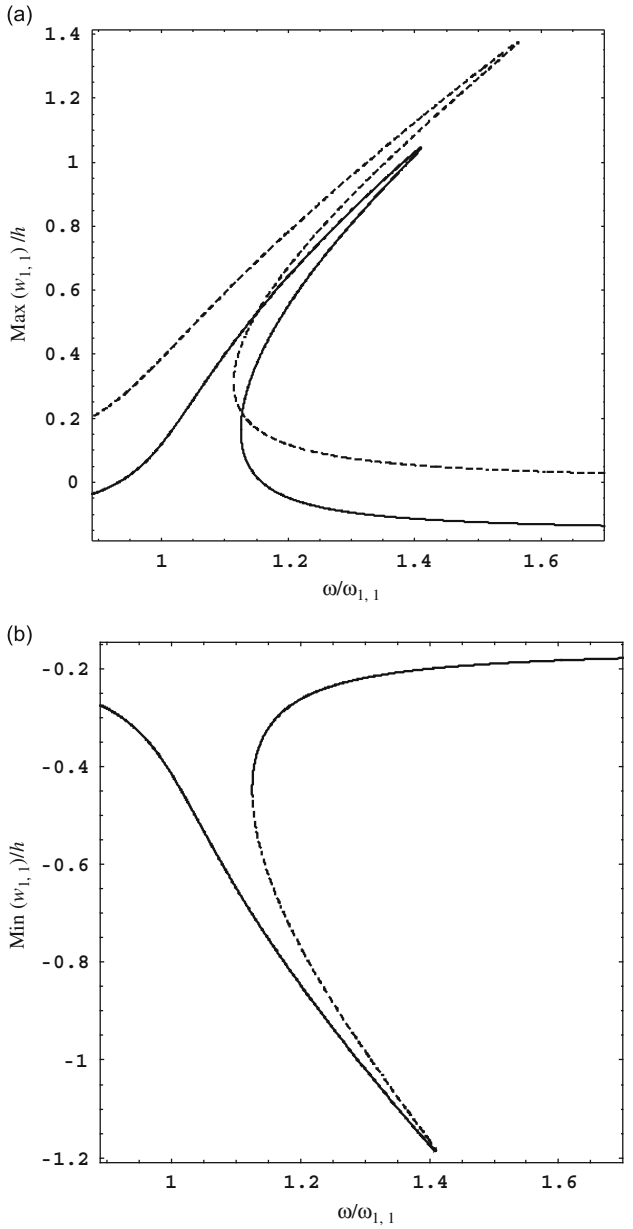

Fig. 7. Comparison of frequency-responses for the main generalized coordinate $w_{1,1}$ with concentrated mass of 0.1 kg with and without gravity; $\zeta_{1,1}$=0.012 and $\tilde{f} = 0.303$ N. (a) Maximum of the generalized coordinate $w_{1,1}$; ▬▬, including vertical gravity; - -, neglecting gravity and (b) minimum of the generalized coordinate $w_{1,1}$ including vertical gravity; ▬▬, stable solution; - -, unstable solution.

4. Conclusions

Results for large amplitude vibrations of rectangular plates carrying a central concentrated mass show that increasing the concentrated mass, the system changes slightly the trend of nonlinearity, specifically decreasing the hardening-type nonlinearity. However, the difference in the trend of nonlinearity is small and this may be useful information when performing experiments on plates using attached sensors (load cell and accelerometer); an added mass is not changing significantly the trend of the nonlinear response if the gravity is not playing a role (vertical plate). Anyway a concentrated mass is amplifying the response at the mass location and is also decreasing the natural frequency.

In case of horizontal plates, gravity may play a significant role in changing the trend of nonlinearity and increasing the natural frequency with respect to the one obtained by neglecting gravity. Moreover, the initial deflection of the plate breaks the symmetry of the response introducing larger deflection inward the bended plate.

Acknowledgements

The author thanks the NSERC of CANADA for his Canada Research Chair (Tier 1) and Discovery Grant, and the Canada Foundation for Innovation for the Leaders Opportunity Fund (LOF).

References

[1] M. Amabili, *Nonlinear Vibrations and Stability of Shells and Plates*, Cambridge University Press, New York, USA, 2008.
[2] M. Sathyamoorthy, Nonlinear vibration analysis of plates: a review and survey of current developments, *Applied Mechanics Reviews* 40 (1987) 1553–1561.
[3] M. Amabili, M. Pellegrini, F. Righi, F. Vinci, Effect of concentrated masses with rotary inertia on vibrations of rectangular plates, *Journal of Sound and Vibration* 295 (2006) 1–12.
[4] D.S. Chiang, S.S.H. Chen, Large amplitude vibration of a circular plate with concentric rigid mass, *Journal of Applied Mechanics* 39 (1972) 577–583.
[5] J. Ramachandran, Nonlinear vibrations of a rectangular plate carrying a concentrated mass, *Journal of Applied Mechanics* 40 (1973) 630–632.
[6] K. Kanaka Raju, Large amplitude vibrations of circular plates carrying a concentrated mass, *Journal of Sound and Vibration* 50 (1977) 305–308.
[7] B.M. Karmakar, Nonlinear vibrations of orthotropic plates carrying concentrated mass, *Journal of Engineering for Industry* 100 (1978) 293–294.
[8] B.M. Karmakar, Amplitude-frequency characteristics of non-linear vibrations of clamped elliptic plates carrying a concentrated mass, *International Journal of Non-Linear Mechanics* 13 (1979) 351–359.
[9] B. Banerjee, Large amplitude vibrations of a clamped orthotropic square plate carrying a concentrated mass, *Journal of Sound and Vibration* 82 (1982) 329–333.
[10] P.A.A. Laura, R.H. Gutiérrez, Comments on "large amplitude vibrations of a clamped orthotropic square plate carrying a concentrated mass", *Journal of Sound and Vibration* 99 (1985) 139.
[11] B. Banerjee, Author's reply, *Journal of Sound and Vibration* 99 (1985) 139.
[12] R.H. Gutiérrez, P.A.A. Laura, Effect of a concentrated mass on large amplitude, free flexural vibrations of elastic plates and beams, *Applied Acoustics* 17 (1984) 135–151.
[13] P.C. Dumir, Y. Nath, M.L. Gandhi, Nonlinear axisymmetric transient analysis of orthotropic thin annular plates with a rigid central mass, *Journal of Sound and Vibration* 97 (1984) 387–397.
[14] S.K. Ghosh, Large amplitude vibrations of an orthotropic right angled isosceles triangular plate carrying a concentrated mass, *Mechanics Research Communications* 14 (1987) 331–339.
[15] C.L.D. Huang, H.S. Walker Jr., Nonlinear vibration of a hinged circular plate with a concentric rigid mass, *Journal of Sound and Vibration* 126 (1988) 9–17.
[16] C.L.D. Huang, S.T. Huang, Finite element analysis of nonlinear vibration of a circular plate with a concentric rigid mass, *Journal of Sound and Vibration* 131 (1988) 215–227.
[17] S. Huang, Nonlinear vibration of a hinged orthotropic circular plate with a concentric rigid mass, *Journal of Sound and Vibration* 214 (1998) 873–883.
[18] S.-R. Li, Y.-H. Zhou, X. Song, Nonlinear vibration and thermal buckling of an orthotropic annular plate with a concentric rigid mass, *Journal of Sound and Vibration* 251 (2002) 141–152.
[19] D.A. Khodzhaev, B.Kh. Éshmatov, Nonlinear vibrations of a viscoelastic plate with concentrated masses, *Journal of Applied Mechanics and Technical Physics* 48 (2007) 905–914.
[20] S. Ilanko, Existence of natural frequencies of systems with artificial restraints and their convergence in asymptotic modelling, *Journal of Sound and Vibration* 255 (2002) 883–898.
[21] E.J. Doedel, A.R. Champneys, T.F. Fairgrieve, Y.A. Kuznetsov, B. Sandstede, X. Wang, *AUTO 97: Continuation and Bifurcation Software for Ordinary Differential Equations (with HomCont)*, Concordia University, Montreal, Canada, 1998.
[22] M. Amabili, Nonlinear vibrations of rectangular plates with different boundary conditions: theory and experiments, *Computers and Structures* 82 (2004) 2587–2605.